The antibacterial properties of branched peptides based on poly(l-arginine): In vitro antibacterial evaluation and molecular dynamic simulations

Lebaudy Eloïse, Lauriane Petit, Yves Nominé, Béatrice Heurtault, Inès Ben Hadj Kaddour, Bernard Senger, Jennifer Rodon Fores, Nihal Engin Vrana, Florent Barbault, Philippe Lavalle

The antibacterial properties of branched peptides based on poly(L-arginine): in vitro antibacterial evaluation and molecular dynamic simulations

Eloïse Lebaudy, Lauriane Petit, Yves Nominé, Béatrice Heurtault, Inès Ben Hadj Kaddour, Bernard Senger, Jennifer Rodon Fores, Nihal Engin Vrana, Florent Barbault[¶], Philippe Lavalle[¶,]*

Dr. E. Lebaudy, L. Petit, Inès Ben Hadj Kaddour, Dr. B. Senger, Dr. J. Rodon Fores, Dr. P. Lavalle

Institut National de la Santé et de la Recherche Médicale, Inserm Unit 1121 Biomaterials and Bioengineering, Centre de Recherche en Biomédecine de Strasbourg, Strasbourg, France

Université de Strasbourg, Faculté de Chirurgie Dentaire, Strasbourg, France

Dr. F. Barbault

Université Paris Cité, CNRS, ITODYS, F75013 Paris, France;

Dr. Y. Nominé

Institut de génétique et de biologie moléculaire et cellulaire, IGBMC, Illkirch, France

Pr. B. Heurtault

Université de Strasbourg, Centre national de la recherche scientifique (CNRS), Laboratoire de Conception et Application de Molécules Bioactives UMR 7199, Faculté de Pharmacie, Illkirch, France

Dr. E. Vrana, L. Petit, Inès Ben Hadj Kaddour, Dr. P. Lavalle

SPARTHA Medical, Centre de Recherche en Biomédecine de Strasbourg, Strasbourg, France

Université de Strasbourg, Faculté de Chirurgie Dentaire, Strasbourg, France

¶These authors contributed equally to this work.

*Corresponding author

E-mail: philippe.lavalle@inserm.fr

Keywords multiple antigenic peptides, molecular simulation, poly(arginine), antimicrobial peptides

Abstract

The emergence of bacterial strains resistant to antibiotics is a major issue in the medical field. Antimicrobial peptides are widely studied as they do not generate as much resistant bacterial strains as conventional antibiotics and present a broad range of activity. Among them, the homopolypeptide poly(L-arginine) presents promising antibacterial properties, especially in the perspective of its use in biomaterials. Linear poly(L-arginine) has been extensively studied but the impact of its 3D structure remains unknown. In this study, the antibacterial properties of newly synthesized branched poly(L-arginine) peptides, belonging to the family of multiple antigenic

peptides, are evaluated. First, *in vitro* activities of the peptides shows that branched poly(L-arginine) is more efficient than linear poly(L-arginine) containing the same number of arginine residues. Surprisingly, peptides with more arms and more residues are not the most effective. To better understand these unexpected results, interactions between these peptides and the membranes of Gram positive and Gram negative bacteria are simulated thanks to molecular dynamic. It is observed that the bacterial membrane is more distorted by the branched structure than by the linear one and by peptides containing smaller arms. This mechanism of action is in full agreement with *in vitro* results and suggest that our simulations form a robust model to evaluate peptide efficiency towards pathogenic bacteria.

Introduction

Health-care associated infections (HAIs) are a major issue in the medical field. Indeed, according to Centers for Disease Control and Prevention (CDC), each year in the USA, 3 % patients develops nosocomial infections [1]. These infections are responsible for 72 000 deaths per year in the USA [2]. To decrease the risk of infections, antibiotics are delivered to patients. Today, the use of conventional antibiotics is the major way to prevent and to fight against bacterial infections. However, in the last decades, some limitations to their use have appeared. Some strains of bacteria developed resistance to conventional antibiotics and in 2019 a study on 25 countries and territories showed that methicillin-resistant *S. aureus* represent about 12% of the *S. aureus* strain and antibiotic resistant *E. coli* is about 36% of the *E. coli* strain. [3] The CDC estimates that infections associated with multi-antibiotic resistant bacteria caused more than 29 000 deaths in 2020 [1]. Thus, conventional antibiotics are no longer effective on some strains that are more and more resistant to them [4]. Thus, finding new strategies and new molecules which would not induce bacteria mutation into resistant strains is very important for the medical field. Different strategies

to decrease the use of conventional antibiotics are studied such as dynamic therapies and the design of new antimicrobial candidates[5].

Antimicrobial peptides (AMPs) are, for example, a class of molecules studied to replace or decrease the use of conventional antibiotics. AMPs are natural small molecules from the innate immunity. Their role is to fight against first microbial invasion [6]. These peptides are most of the time cationic and amphipathic and present a broad spectrum of antimicrobial properties, namely antibacterial, antifungal and antiviral activities [7, 8]. A lot of studies detailed that the antibacterial activity of AMPs was due to the interaction between positive charges of the AMPs and negative charges of the outer membranes of bacteria. Indeed, due to these electrostatic interactions, the polycation can be adsorbed to the bacterial membrane. Then, other interactions such as hydrophobic interactions lead to the deformation of the membrane and the formation of pores [9-11].

Among AMPs, antimicrobial peptides with branched globular structures around a core, also called dendrimers, are highly studied to fight against multidrug resistant bacteria [12-14]. For example, Siriwardena *et al*. showed the strong antimicrobial properties of an AMP dendrimer due to its higher density of functional groups in interaction with the surface of the bacteria [14]. Besides, AMP dendrimers present a 3D structure which seems to favor the access of all the functions of the molecules to the bacterial membrane. Thus, these molecules can be effective for bacterial inhibition and other properties can be matched to focus on several applications, such as biofilm prevention, cancer treatment, intracellular delivery, cell transfection… by adding active molecules on the branched structure [15-17]. Moreover, the use of dendrimeric structures enables the optimization of their stability by avoiding their degradation by protease for instance, leading to better antimicrobial activity [18].

We demonstrated recently that homopolypeptides as polycations are a promising tool to fight against bacteria and can be used to design antimicrobial coatings [19]. These polymers are positively charged, enabling them to interact with and destabilize negatively charged bacterial membranes. Finally, these polycations can be associated to a negatively charged polymer to develop a coating with longer release of antibacterial properties [20]. In these studies, strong antibacterial properties were conferred to the coatings by the use of a linear homopolypeptide, poly(L-arginine) (PAR). pKa of arginine is of 12.5 and thus all residues will be protonated in physiological conditions (*i.e.* pH from 2 to 8.5 in the body). This is one of the main advantages of the polyarginine peptides, they are always charged and thus they strongly interact with negatively charged bacterial membranes and they finally destabilize them. By using only PAR associated with hyaluronic acid in a layer-by-layer buildup process, a thin coating can be produced on all surfaces. This leads to a "multilayer" film with the ability to prevent colonization by any kind of bacteria. Moreover, we showed that the size of the PAR chain (number of arginine residues per chain) play a key role on the antibacterial properties of the coating [21]. Indeed, the antibacterial properties are related to the diffusion of the PAR chains inside the multilayer of polyelectrolytes. This mobility determines their ability to be available on the surface and to adsorb on the membrane of the incoming bacteria. Finally, small chains can better diffuse inside the film compared to longer one. However, too small chains produce thinner films. Thus, the antimicrobial activity of the coating is based on a tradeoff between mobility of the PAR chains and their ability to produce thick films. The results show that the PAR with 30 residues (PAR30) is the optimal chain length range to design efficient coatings.

From these results, the next question is if the size of the PAR chains is the unique parameter tuning the antibacterial properties or if the 3D structure of the PAR can also influence the

antimicrobial properties of this molecule. For example, cyclic antimicrobial peptides seem interesting as some studies present the stronger antibacterial activity but also a higher resistance to degradation of the cyclic structure compared to a linear one [22, 23]. Besides, peptide dendrimers are interesting structures and some of them have been described to possess strong antibacterial activities. Thus, we decided to study multiple antigenic peptides (MAPs) of arginine amino acids. MAPs are synthetic branched peptides that can be compared to dendrimers because of their structure. MAPs were already studied for various applications such as diagnostics, antiviral and vaccines strategies but there were only few studies on their antibacterial properties [24-27]. Indeed, MAPs are based on a lysine tree structure which provides the core of the dendrimer structure. In some applications, these structures have shown to improve the immunogenic response and they can also improve the diagnosis performance [27]. Finally, they can be easily tuned and functionalized with various amino acid sequences. In the present study, we designed MAPs based on arginine residues with a lysine core. As lysine possesses two amine groups, two amino acids can be attached to one lysine on the amine groups. In this way, multibranched molecules can be designed through relative simple peptidic synthesis routes. It is then possible to develop MAPs with different numbers of arms depending on the number of lysine residues used in the core. Thereby we can obtain molecules comprising only arginine in the arms but distinguished by their configurations, as presented in **Figure 1**. For the nomenclature, the peptide composed of 4 arms with 5 or 8 arginine residues per arm was named respectively R5MAP4 and R8MAP4 (**Figure 1.B**) and the peptide composed of 8 arms with 5 or 8 arginine residues in each arm was named respectively R5MAP8 and R8MAP8 (**Figure 1.C**). A cyclic peptide containing 10 arginine residues was also produced (cyclo (R10)). A linear peptide called R20 was added as a control and was composed of 20 arginine residues (**Figure 1.A**). In our previous studies [20, 21], a linear

peptide with 30 arginine residues (PAR30) was the most widely used arginine homopolypeptide but in the present study our aim was to compare the R5MAP4 with a linear peptide containing the same number of arginine residues, instead of PAR30, so R20 was selected.

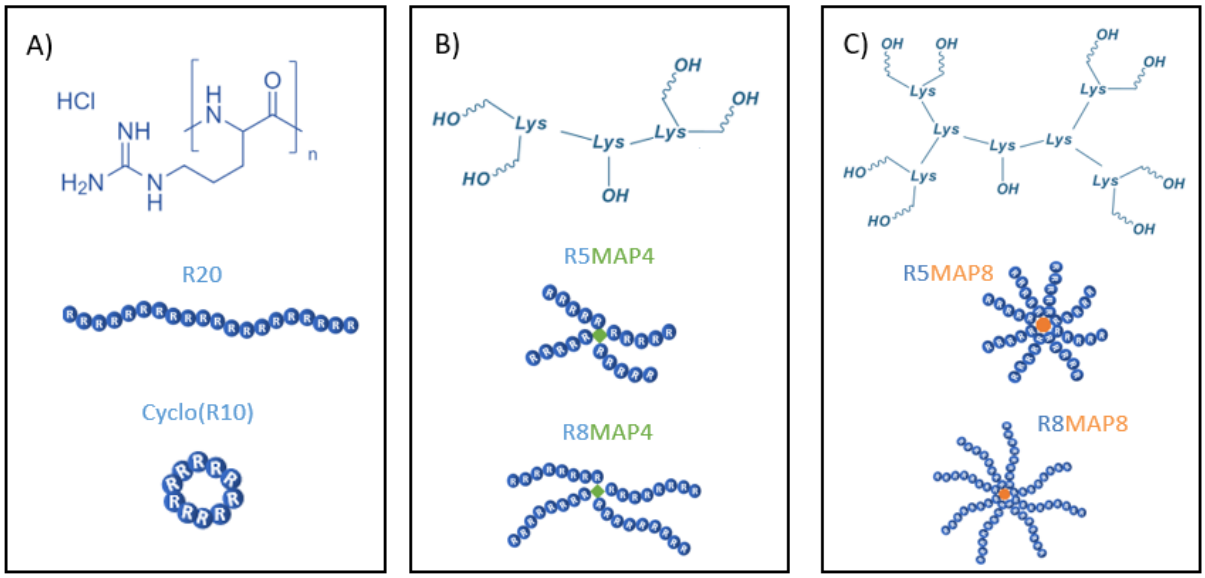

Figure 1. Chemical developed formula and schemes of various polyarginine peptidic structures: linear and cyclo poly (L-arginine) peptides (A), 4-arm Multiple Antigenic Peptides (MAP4) (B), 8-arm Multiple Antigenic Peptides (MAP8) (C).

In this study we evaluated antimicrobial activities of these MAPs towards Gram positive and Gram negative bacteria and we compared these activities with that of a linear PAR composed of 20 arginine residues (R20). Biocompatibility, pro- or anti-inflammatory properties were also evaluated. Then, to better understand the experimental results obtained and the mechanism involved, molecular simulation was performed which monitors the interactions between the different peptides and the bacterial membrane. This method enables to provide a good understanding of the mechanism involved between peptides and bacterial membranes.

1. Materials and methods

1.a. Materials

R5MAP4 (Mw=3526.80 kDa, purity 95.0 %), R8MAP4 (Mw=5401.20 kDa, purity 95.8 %), R5MAP8 (Mw=7163.40 kDa, purity 98.12 %), R8MAP8 (Mw= 10911.70 kDa, purity 95.07 %), Cyclo(R10) (Mw= 1561.90 kDa, kDa, purity 95.06 %) and R20 (Mw= 3141.95 kDa, purity 93.05 %) already used previously was also purchased from Pepmic and analyzed with HPLC (high performance liquid chromatography) and mass spectroscopy (**Figure S1**). Bodipy™ TR-cadaverine (5-(((4-(4,4-Difluoro-5-(2-Thienyl)-4-Bora-3a,4a-Diaza-s-Indacene-3-yl)phenoxy)acetyl)amino)pentylamine, Hydrochloride) and thiazolyl blue tetrazolium bromide were purchased from ThermoFischer Scientific (USA). Griess reagent, Trizma hydrochloride, Fetal bovine serum, DMSO and lipopolysaccharides from *E. coli* O111:B4 (LPS) were purchased from Merck (USA). *S. aureus* ATCC25923 and *P. aeruginosa* ATCC27853 were used for bacteria tests. DMEM high glucose was purchased from Dutscher (France). Penicillin-streptomycin was purchased from Biowest (France).

1.b. Minimal Inhibitory Concentration evaluation

Minimal Inhibitory Concentration (MIC) was tested on two bacteria strains: *S. aureus* ATCC25923, Gram positive bacteria and *P. aeruginosa* ATCC27853 Gram negative bacteria. To evaluate the MIC of the peptides, the samples were dissolved in milliQ water at concentrations between 5 μg.mL^{-1} and 2 mg.mL^{-1}. A bacterial suspension was prepared at a concentration of 8 × 10^5 CFU.mL^{-1} in Mueller-Hinton Broth (MHB). Then, 90 μL of bacterial suspension were added in each well of a 96-well plate and 10 μL of peptides at the different concentrations were added to the bacteria. Control wells were also prepared by adding 10 μL of antibiotics (tetracyclin at 1

μg.mL^{-1} + cefotaxim at 0.01 μg.mL^{-1}) for negative control or of milliQ water for positive control to the 90 μL of bacterial suspension. Three wells were prepared for each condition. Finally, the plate was incubated for 24 hours at 37°C and the optical density (OD) was measured at 595 nm. The OD of each condition was normalized with respect to the control.

The MIC was evaluated a minimum of three times for each peptide and bacteria strain. Then, the average value for each concentration and the standard deviation were calculated. Sigma plot software was used to plot the normalized bacterial growth (%) as a function of the concentration of peptides and the MIC was determined as the minimal concentration to inhibit 99.9 % of bacteria.

1.c. Kinetics of bacteria kill

To see in detail how fast the peptide is able to kill the bacteria, the number of bacteria in contact with the peptide was followed in time. First, a bacterial suspension was prepared at a concentration of 8×10^5 CFU.mL^{-1} in MHB. In Falcon tubes, 9.9 mL of bacterial suspension were placed. Then, 100 μL of peptide dissolved in milliQ water were added to the bacteria. In this way, the final concentration of the peptide was the MIC of R5MAP4 evaluated previously (10 μg.mL^{-1}). As the MIC in mass was much higher for R8MAP8 than the MIC for R5MAP4 and R20, a second concentration (MIC of R8MAP8 equal to 50 μg.mL^{-1}) was tested. A control Falcon tube was also prepared by adding 100 μL of milliQ water to 9.9 mL of bacterial suspension. The Falcon tubes were incubated at 37°C for 8 hours.

At $t = 0$, 1, 2, 4, 6 and 8 hours, 10 μL of each tube were picked and diluted (from 100 to 10 000 times). 100 μL of each dilution were placed on agars and spread and then incubated at 37°C for 24 hours. After 24 hours, the colonies on agars were counted.

1.d. Fluorescent displacement assay

The interactions between peptides and LPS, which is the major component of Gram negative outer membrane can be observed using Bodipy TR-cadaverine fluorescent dye (Bodipy). The protocol was adapted from Harm *et al*. [28] First, LPS at a concentration of 7.5 μg.mL^{-1} in Tris 50 mM pH 7 buffer (Tris), Bodipy at 2.1 μM in Tris and peptides at concentrations between 5 and 20 μg.mL^{-1} in Tris were prepared. Then, in a black 96-well plate, 50 μL of LPS and 50 μL of Bodipy were added and placed under stirring in the dark for 30 minutes. Then, 100 μL of peptides at the different concentrations were added to the LPS and Bodipy and placed under stirring in dark for 15 minutes. The fluorescence was then measured using a Varioskan spectrophotometer (ThermoFischer, USA) at an excitation wavelength of 590 nm and emission wavelength of 620 nm.

1.e. Cytotoxicity on fibroblasts and macrophages

The cytotoxicity of peptides in solution was tested by measuring the metabolic activity of RAW 264.7 macrophage cells and of BALB/3T3 fibroblast cells by a MTT assay. The experiment was performed following standard ISO 10993-5 norm. In a 96-well plate, 50 000 cells were seeded with DMEM High Glucose with the addition of 5 % low endotoxin serum and 1% PS (DMEM) and incubated for 24 hours at 37°C. After 24 hours, the medium was removed and replaced with peptide dissolved and diluted in DMEM at concentrations between 0.5 and 100 μg.mL^{-1}. Three wells were prepared for each concentration. The cells were incubated 24 hours at 37°C with peptides. The medium was then replaced by MTT at 0.2 mg.mL^{-1} in DMEM and incubated for 3 hours. Finally, the formazan crystals were dissolved in 100 μL of DMSO. The absorbance at 570 nm in each well was measured using a Varioskan spectrophotometer (ThermoFischer, USA).

1.f. Nitric Oxide (NO) quantification with Griess reagent

The anti-inflammatory activities of the R5MAP4 and R20 peptides were evaluated on macrophages by quantifying the nitric oxide (NO) released from them. First, 50 000 RAW 264.7 cells were seeded with DMEM and incubated for 24 hours at 37°C. Then, peptides at a concentration of 20 μg.mL^{-1} were prepared in DMEM and added to the wells for 24 hours. For the control, LPS and IL-4 were used at 10 ng.mL^{-1} in medium. Thus, controls with only LPS or only IL-4 were prepared. Samples with peptides with LPS or peptides with IL-4 were also studied. Three wells were prepared for each condition. We also prepared three wells with cell culture medium only, and three wells with the addition of DMSO to the medium. After 24 hours, 100 μL of each well were placed in another 96-well plate. Then, 100 μL of acetoacetic 0.01 M pH 2.5 buffer and 50 μL of Griess reagent at 6 mg.mL^{-1} were added. The plate was placed under agitation for 5 minutes and the absorbance at 540 nm was measured using a Xenius XC spectrophotometer (SAFAS, Monaco). The absorbance was then normalized with the absorbance of LPS samples.

1.g. Hemolysis

The hemolysis of red blood cells in contact with peptides was also quantified. For this experiment, red blood cells from sheep were washed three times in PBS. 10 mL of red blood cells were placed in two Falcon tubes and 30 mL of PBS were added in each. The cells were centrifuged 5 minutes at 2500 rpm. Then, the supernatant was removed and replaced by 30 mL of fresh PBS and these two first steps were repeated twice. After the washing steps, the red blood cells were diluted in 10 mL of PBS. In a U bottom 96-well plate, 100 μL of red blood cells were poured. Then, 100 μL of peptides at concentrations from 0.6 to 60 μM in PBS were added. For controls, 100 μL of PBS or 100 μL of Triton at 0.1 % in PBS were added to 100 μL of red blood cells. Three wells were prepared for each concentration. The plate was incubated at 37°C for 30 minutes and then centrifuged. 100 μL of the supernatant of each well was poured in a 96-well plate and the

absorbance of the supernatant was measured at 550 nm using Xenius XC spectrophotometer (SAFAS, Monaco).

1.h. Statistical analysis

Each experiment was performed at least three times (except for hemolysis experiment that was performed two times and for the kinetics of bacteria lysis that was performed only one time). The represented results correspond to the average of independent experiments and the error bars represent standard error of the mean. The One-Way ANOVA on Ranks statistical test was performed using Sigma Plot software to reveal significant differences between peptides. If the *p*-value is lower than 0.05, the different conditions were considered significantly different.

1.i. Molecular dynamics simulations

Molecular modeling was conducted with the GPU version of Amber 20 software package. [29] To generate branched peptides, slight modifications of the lysine residue were made and their partial atomic charges were determined through the semi-empirical QM computations AM1-BCC [30]. All molecular dynamics (MD) simulations were conducted in water boxes under NTP conditions and used the protein force-field ff14SB in conjunction with gaff2 for the modified lysine residues. When membrane systems were considered the lipid21 force-field were added to the systems [31-34]. Bacterial membranes were created for *P. aeruginosa* (PA) and *S. aureus* (SA) through the CHARMM-GUI interface [35]. A lipid ratio of 23% 1,2-dipalmitoyl-sn-glycero-3-phosphoethanolamine (DPPE), 46% of 1,2-dioleoyl-snglycero-3-phosphoethanolamine (DOPE) and 31% of 1,2-dipalmitoyl-sn-glycero-3-phosphoglycerol (DPPG) was generated for PA while a ratio of 70% of 1,2-Dioleoyl-sn-glycero-3-phosphocholine (DOPC) and 30% of 1,2-Dioleoyl-sn-glycero-3-phospho-rac-(1-glycerol) (DOPG) was chosen for SA [36, 37]. Molecular schemes of these lipids are displayed in **Figure S3**.

The protocol of MD simulations starts with a first minimization of the system followed by a heating phase to reach the desired temperature of 300K. For peptides alone in water, trajectories of 40 ns were generated and repeated 4 times (replicas). Both membrane systems were firstly equilibrated alone in water through 1.2 μs of MD. Six peptide/membrane complexes were constructed by placing either the R20, R5MAP4 or R8MAP8 peptides above PA or SA equilibrated membrane surfaces at a distance of about 50 Å authorizing the peptides to freely rotate or reorganize before making adsorption on membranes. MD were then realized for these systems for 1.2 μs for each system. 4 replicas were generated to provide meaningful statistical analyses which were performed with the cpptraj module of Amber [38]. All structural visualization and images were created with the VMD software [39].

2. Results and discussion

2.a. Antimicrobial properties of peptides

2.a.1. Minimal inhibitory concentrations (MIC)

The minimal inhibitory concentrations (MIC) of peptides in solution on both Gram positive *S. aureus* and Gram negative *P. aeruginosa* bacteria, two of the main bacteria responsible for nosocomial infections, are shown on **Figure 2**. First, one cyclo arginine and four MAPs were compared to a linear PAR. Results showed that the cyclo(R10) did not present any antibacterial activity on both *S. aureus* and *P. aeruginosa*. Besides, R8MAP4 and R5MAP4 have higher antibacterial activity with a lower MIC compared to R5MAP8 or R8MAP8.

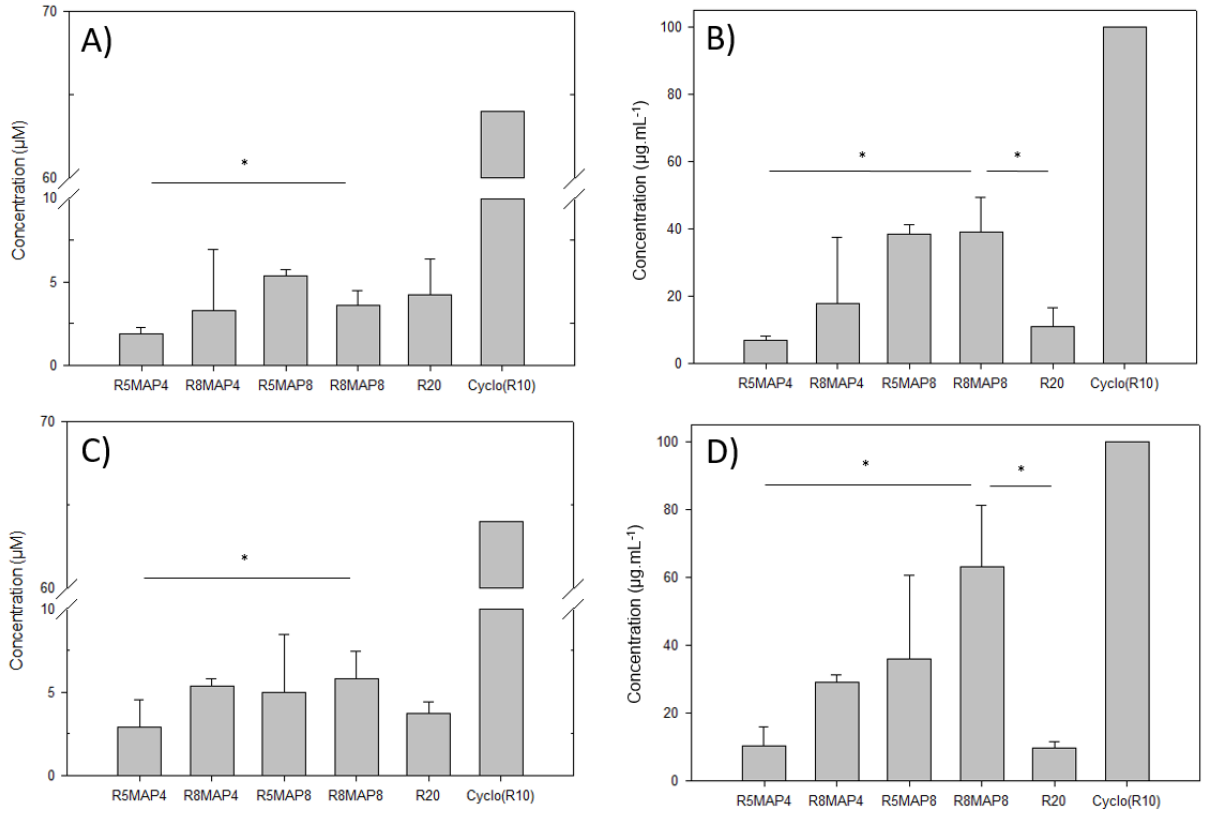

Figure 1. Minimal Inhibitory Concentration (MIC) of R5MAP4, R8MAP4, R5MAP8, R8MAP8, R20 and Cyclo(R10) poly(L-arginine) peptides in solution with S. aureus ATCC25923 in μM (A), or in μg.mL^{-1}(B) and with *P. aeruginosa* ATCC27853 in μM (C) or in μg.mL^{-1} (D). The MIC determination was measured in three wells, and the experiment was repeated 3 times in an independent way. The MIC was calculated as the concentration to inhibit 99.9% of the bacteria. The graphs show averages of the three experiments with error bars representing the standard error of the mean. * $p < 0.05$.

Thus, for all the further experiments we will focus on two MAPs, the smaller one and most effective, and the larger one, *i.e.*: R5MAP4 and R8MAP8, respectively. We will compare the results with a linear PAR composed of 20 arginine residues (R20). R5MAP4 presented the smallest MIC on *S. aureus* with a value of 1.9 ± 0.4 μM (or 6.8 ± 1.2 μg.mL^{-1}). Besides, the MIC on *S. aureus* of the linear homopolypeptide R20 was higher (4.3 ± 2.1 μM (or 11 ± 6 μg.mL^{-1}) and the

MIC of R8MAP8 on *S. aureus* was 3.6 ± 0.9 μM (or 49 ± 27 μg.mL^{-1}). This suggests that for an equal number of arginine residues (20), a branched configuration of polyarginine is more effective to inhibit the growth of *S. aureus* than the linear one. However, in an unexpected way, increasing the number (from 4 to 8) and length of arms (from 5 to 8) of MAPs leads to a slight but significant decrease in the antimicrobial activity of the chains. On *P. aeruginosa,* the MIC of R8MAP8 (5.8 ± 1.7 μM or 63 ± 18 μg.mL^{-1}) was higher than the MIC of R20 and R5MAP4. In contrast, R20 (3.7 ± 0.6 μM or 9.6 ± 1.9 μg.mL^{-1}) and R5MAP4 (2.9 ± 1.7 μM or 11 ± 6 μg.mL^{-1}) showed roughly the same values. To compare these results with a well-established drug, we performed MIC evaluation in the same conditions with LL-37, one of the most known human antimicrobial peptides (**Figure S2**).

Thus, the MIC in mass of R8MAP8 on *P. aeruginosa* was 6 times higher than the MIC of R5MAP4 or R20. We did not expect such a result. Initially, we assumed that the key parameter in the activity is the primary sequence, *i.e.* the number of positive charges that increases with the number of arginine residues on the chain, leading to more interactions between the PAR and the bacterial membrane. R8MAP8 is composed of 64 arginine residues and R20 and R5MAP4 of only 20 arginine residues. Thus, we expected that R8MAP8 would have the best antimicrobial properties with the smallest MIC due to its high number of positive charges. However, the highest MIC and thus the lowest activity is observed for the R8MAP8 peptide. We can make the assumption that the structure of R8MAP8 has strong steric hindrance and/or that there is charge repulsion within the peptide. Thus, all the charges are probably not in close vicinity to the bacterial membrane. R5MAP4 with a lower number of arms and shorter ones is probably less affected by steric hindrance. Molecular simulations will be performed in the second part of this study to have a better view of the conformation of the different peptides and to confirm this hypothesis.

2.a.2. Kinetics of bacteria lysis

Further experiments were performed to refine the difference in antibacterial activities of the three peptides, R20, R5MAP4 and R8MAP8. We first evaluated the kinetics of *S. aureus* lysis by monitoring the evolution of the number of bacteria over time for the first 8 hours of culture (time-kill curves). Living colonies were counted after seeding on agar plates. **Figure 3** shows the results for the three peptides incubated at a concentration of 10 μg.mL^{-1} for R20, R5MAP4 and at 10 and 50 μg.mL^{-1} for R8MAP8. Data were normalized by using as reference (100%) the number of colonies at the beginning of the kinetics. First, we observed that the number of colonies over time decreased and reached zero after 8 hours for R20 and R5MAP4. This decrease was expected, as 10 μg.mL^{-1} corresponds to the MIC. However, the profile of decrease was not similar for R20 and R5MAP4. Indeed, the decrease in colonies was about 70% after one hour in culture with R5MAP4. By contrast, with R20, the number of bacteria increased up to 120% during the two first hours of the experiment and then decreased in the same manner than R5MAP4 after 4 hours, before reaching slowly zero after 8 hours. The kinetics of bacteria lysis with R5MAP4 is the fastest. Besides, the number of colonies over time for R8MAP8 at 10 μg.mL^{-1} first decreases but after 6 h, an increase of the number of colonies is noticed. This increase was expected as the MIC is above 10 μg.mL^{-1} for R8MAP8. Indeed, peptides probably stays in contact with the bacterial membrane after lysis so it becomes less and less available under time.

Thus, all these results suggest that the activity of peptides, at a concentration to 10 μg.mL^{-1}, is stronger for R5MAP4 than for R20 or R8MAP8. A second concentration for R8MAP8 of 50 μg.mL^{-1} was studied, closer to the MIC value of this peptide. A faster decrease in the number of colonies was observed for R8MAP8 at 50 μg.mL^{-1} compared to 10 μg.mL^{-1} with about 100% of

decrease after 1 hour of incubation, which shows that the increase noticed at the end of the time-kill curve for 10 μg.mL^{-1} is clearly due to the low concentration of R8MAP8.

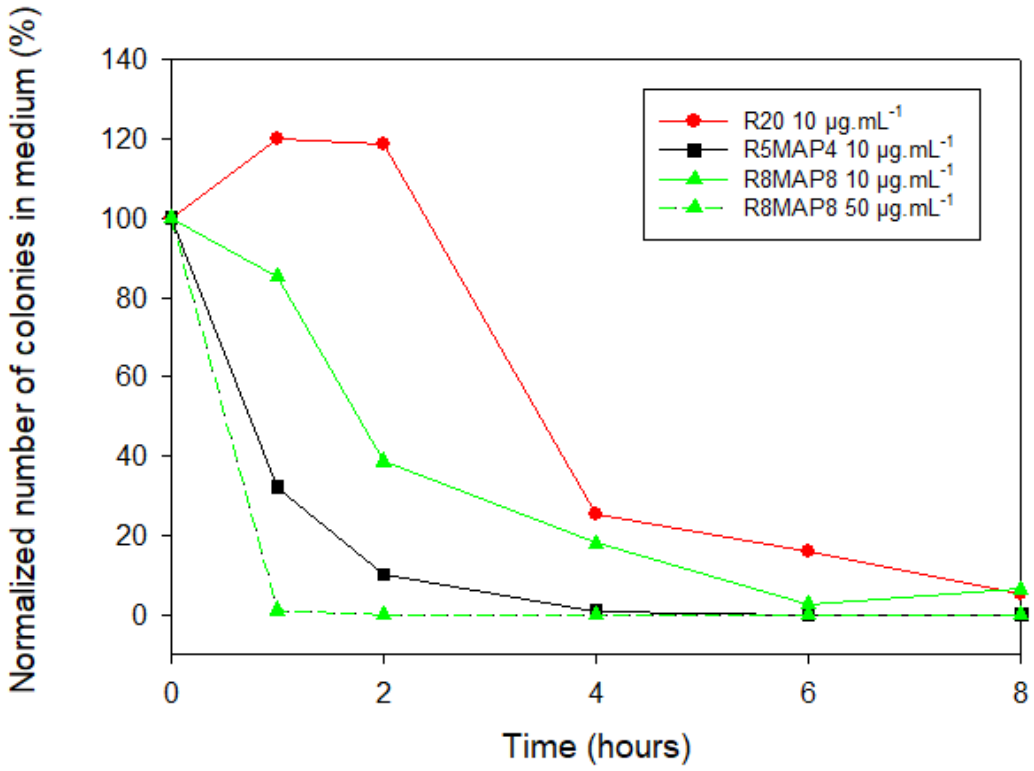

Figure 2. Evolution of the number of colonies of S. aureus ATCC25923 as a function of time during incubation with R20, R5MAP4 and R8MAP8 peptides. The kinetics of bacteria lysis was tested at 10 μg.mL^{-1} for R20 and R5MAP4 peptides and at 10 and 50 μg.mL^{-1} for the R8MAP8 peptide. The number of bacteria colonies was counted on agar plates after 24 hours of culture. Two agars plates were prepared and counted for all conditions at each different time. The results were normalized by the number of bacteria added to the medium at the beginning of the experiment.

2.a.3. Interaction between peptides and LPS from bacterial membrane

To better understand the peptide antimicrobial mechanism, the interaction between lipopolysaccharide (LPS), which is a major molecule of the outer bacterial membrane (mainly Gram negative) protecting the bacteria from its environment and stabilizing its structure, and R20,

R5MAP4 and R8MAP8 peptides at different concentrations has been studied using a fluorescent displacement assay (**Figure 4**). For this experiment, Bodipy TR-cadaverine fluorescent dye was used. This dye binds to LPS leading to fluorescence quenching. Then, the peptides were added to the LPS / Bodipy TR-cadaverine mixture. The interactions between the peptides and the LPS were quantified by measuring the fluorescence recovery of the Bodipy TR-cadaverine. As depicted in **Figure 4**, we observed a fluorescence increase with the addition of every peptides even at 5 μg.mL^{-1}. This means that the three peptides are able to make strong interactions with LPS. For concentrations higher than 5 μg.mL^{-1}, a plateau is reached for the three peptides and no significant difference was observed in fluorescence between them, indicating that they were bound to the LPS in the same manner. These interactions were expected according to the literature [40]. Indeed, cationic peptides and polymers can bind to the bacterial membranes due to electrostatic interactions between their positive charges and the negative charges of the bacterial membranes, and in particular due to the presence of negatively charged LPS chains in the membranes.

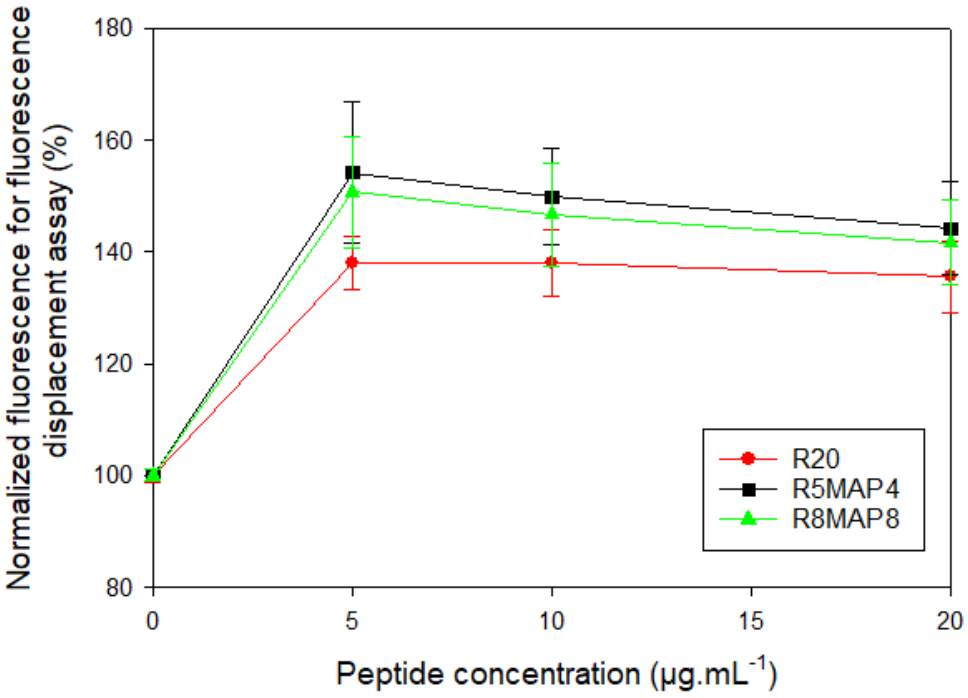

Figure 3. Interactions between LPS from bacterial membrane of E. coli and R20, R5MAP4 and R8MAP8 peptides using fluorescent displacement assay. The Bodipy TR-cadaverine fluorescent dye was quenched by the LPS. The fluorescence increase is directly related to the interaction between LPS and peptides once the peptide was added (t = 0). The results were normalized with the fluorescence in the absence of peptide in the solutions. All conditions were tested independently three times. The results show the averages of these three experiments and the error bars represent standard error of the mean.

2.b. Biocompatibility of the peptides

2.b.1. Cytotoxicity

We then determined the cytotoxicity of peptides in solution on BALB/3T3 fibroblast cells and on RAW 264.7 macrophage cells by quantifying the metabolic activity of cells with MTT assay when cells are incubated for 24h with peptides at various concentrations. The results on fibroblasts were presented in **Figure 5.A**. R20 and R5MAP4 were non cytotoxic on fibroblasts even at 100 μg.mL^{-1} whereas R8MAP8 showed cytotoxicity at concentrations equal or higher than 50 μg.mL^{-1}, which is also the MIC of the peptide on *S. aureus* and *P. aeruginosa*. Due to these results, the use of this R8MAP8 peptide for medical applications can be problematic. Cytotoxicity on macrophage cells was also tested to evaluate a potential role of peptides on the inflammation processes (pro- or anti-inflammatory properties) (**Figure 5.B.**). We observed that R5MAP4, R20 and R8MAP8 showed no cytotoxicity on macrophages up to 100 μg.mL^{-1} In the presence of peptides, the metabolic activity of macrophages cells remains higher than 70% which is the critical value below which the standard ISO 10993-5 considers the compound cytotoxic. Finally, one may notice the excellent value of at least 10 for the ratio between the cytotoxic concentrations (for both fibroblasts and macrophages) and the MIC values (less than 10 μg.mL^{-1} for R5MAP4 and R20, as

presented in **Figure 2**). Both peptides could be efficient to prevent or fight infections without being toxic for eukaryotic cells.

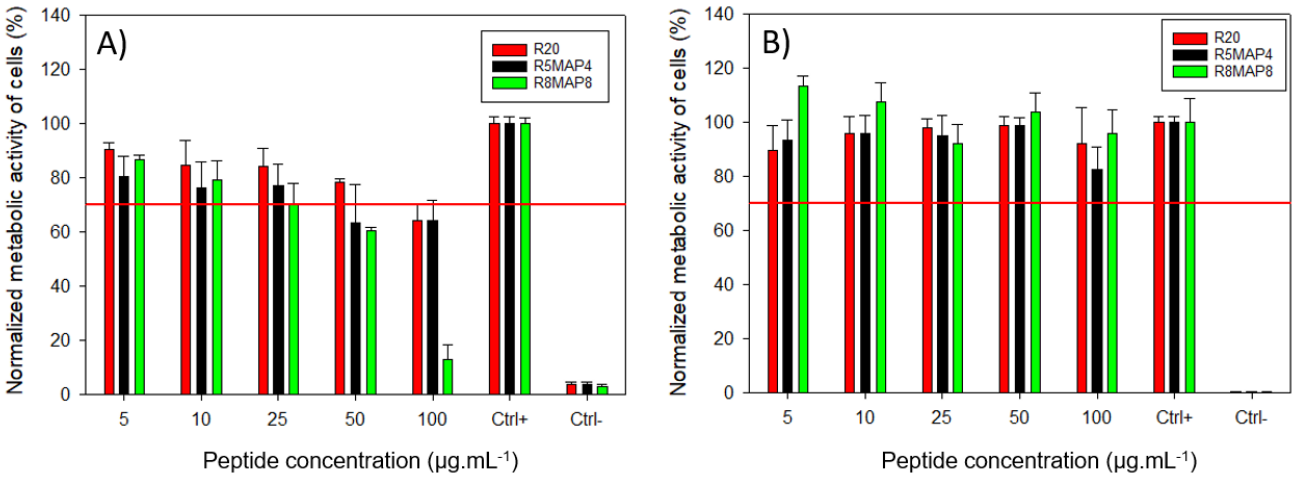

Figure 4. Normalized metabolic activity of BALB/3T3 fibroblasts (A) and RAW264.7 macrophages (B) with different concentrations of the R20, R5MAP4 and R8MAP8 peptides. The results were normalized with a control using cells in cell culture medium only (without peptides). The red line corresponds to the metabolic activity equal to 70%, which is the minimal metabolic activity to consider a material non-cytotoxic regarding to the ISO10993-5 norm. The results present averages over 3 experiments with the error bars representing the corresponding standard errors of the mean.

2.b.2. NO quantification

After demonstrating that the peptides are not cytotoxic on RAW 264.7 macrophages, the NO released by these cells was quantified. NO is known to be released only when macrophages were polarized into M1 pro-inflammatory macrophages. Thus, if the peptides induce an increase in the NO secretion, it means that they could promote the inflammation process. First, addition of R20 (**Figure 6A**), R5MAP4 (**Figure 6B**) or R8MAP8 (**Figure 6C**) to the medium did not significantly increase the NO secretion compared to the control with culture medium only. First, no significant

difference is observed between IL-4-enriched medium condition and with only peptides added to the medium. Thus, peptides do not differentiate the macrophages into M1 phenotypes. Then, as expected, stimulation of macrophages with LPS strongly increases the NO level by inducing a pro-inflammatory response. When the peptide R5MAP4 was added to the medium in the presence of LPS, a slight decrease of the NO level was observed compared to the LPS control. However, for the medium containing the R8MAP8 or R20 peptides added to LPS, a large and significant decrease of the NO released was noted compared to the LPS control. This result suggests that R20 and R8MAP8 have anti-inflammatory properties. The anti-inflammatory property of polyarginine with 30 residues (R30) was already described [41, 42]. Thus, these results are in agreement with previous results. Besides, as presented in **Figure 4.** the peptides interact with LPS. Thus, peptides might be attenuating the action of LPS which can also explain the results observed in **Figure 6**.

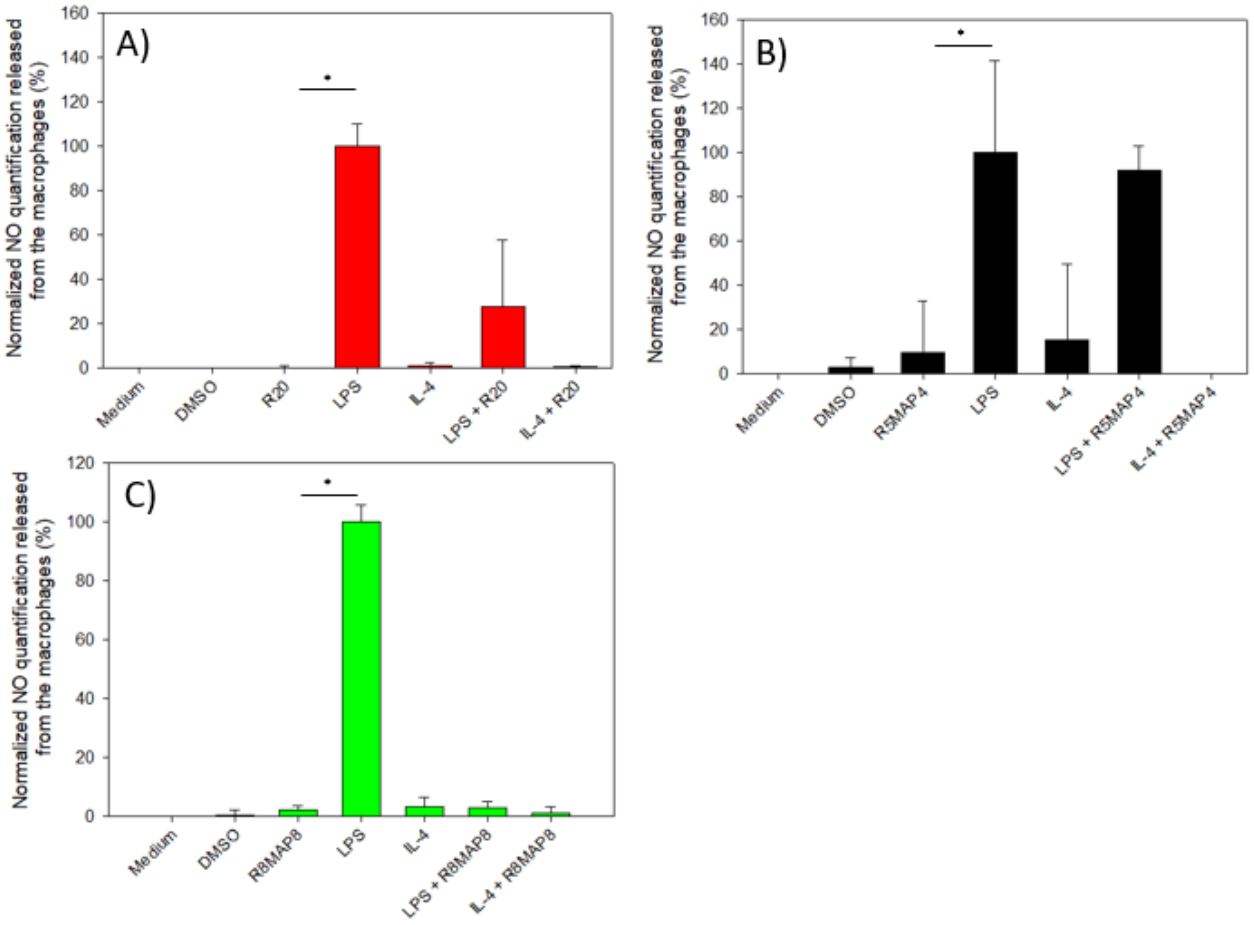

Figure 5. Quantification of the NO secretion from RAW2674.7 macrophage cells in contact with the R20 (A), R5MAP4 (B) and R8MAP8 (C) peptides. The results were normalized with the NO quantity secreted by the cells in LPS-enriched cell medium. For the three experiments, different controls were considered: one with cells in cell culture medium, one with cells in DMSO enriched medium as a control to see the NO secreted by dead cells, other with LPS or IL-4 enriched medium. Moreover, the NO secreted by cells after 24 h of treatment with the different peptides and with a combination of the peptides with LPS / IL-4 was quantified. Three independent experiments were performed, with three values measured in each experiment. The graph represents averages and error bars represent standard error of the mean. * $p < 0.05$.

2.b.3. Non hemolytic properties

The influence of the MAP peptides on red blood cells and on their hemolysis was evaluated as another biocompatibility test. The results in μg.mL^{-1} are depicted in **Figure 7** and in μM in **Figure S3**. R8MAP8 shows higher hemolytic properties than R5MAP4 or R20. Indeed, 20% of red blood cells are being lysed with R8MAP8 at a concentration of 40 μg.mL^{-1} and 80% of them at a concentration of 80 μg.mL^{-1}. For cells treated with R5MAP4 or R20, the hemolysis is null at 40 μg.mL^{-1} and lower than 10% at a concentration of 80 μg.mL^{-1}. These results can be correlated with the aforementioned cytotoxicity of the peptides (**Figure 5**) where R8MAP8 was highly cytotoxic on fibroblasts at concentrations higher than 50 μg.mL^{-1}. In contrast, both R5MAP4 and R20 showed no cytotoxicity towards fibroblasts in solution, even at 100 μg.mL^{-1}.

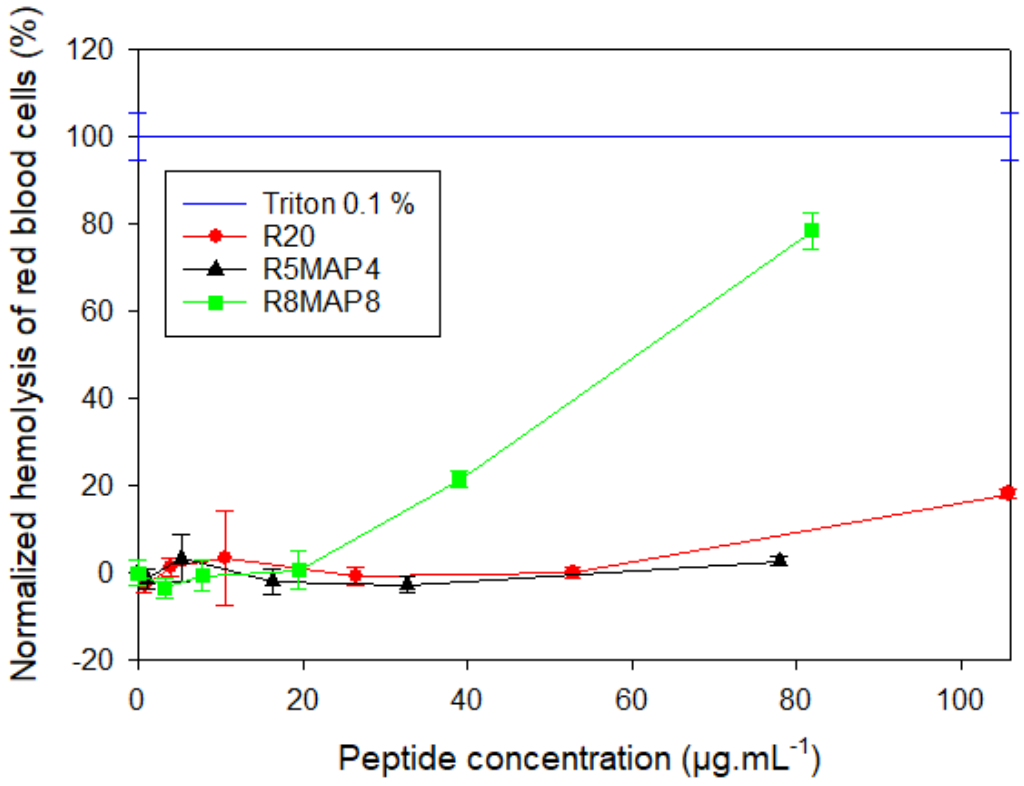

Figure 6. Percentage of hemolysis of a red blood cell population due to the addition of R20, R5MAP4 or R8MAP8 at various concentrations (μg.mL^{-1}). The results were normalized with a control in which red blood cells were placed in Triton 0.1 %. 100% of hemolysis was obtained

with a control in which cells were treated with Triton 0.1 %. The experiments were recorded three time in an independent manner, with three measures for each condition in every experiment. The data points in the graph represents averages and error bars represent standard errors of the mean.

2.c. Computational studies

These *in vitro* results showing higher antibacterial properties for R5MAP4 compared to R8MAP8 were not fully expected since our hypothesis was that increasing the number of arginine units and the number of arms of the MAP will increase the antibacterial properties. To better understand these observations, molecular simulations have been performed. First, the conformation of the peptides was studied and then the adsorption of the peptide to the bacterial membrane and the interactions between both were simulated. Thus, molecular dynamics simulations were employed to explore the conformations of these peptides in aqueous environment and their behavior in the vicinity of bacterial membranes, with the aim of elucidating their ability to interact and disrupt such membranes. The peptides R5MAP4, R8MAP8 and R20 exhibit diverse activities, warranting an investigation of their structure-activity relationships.

2.c.1. Peptides alone

Examination of molecular dynamics trajectories for the three peptides indicates a lack of stable structural organization, with no discernible presence of secondary structure elements typically observed in proteins. These observations are in line with the three peptides' inherent topological characteristics, sizes, and charges.

The visualization of the trajectories has revealed a globular shape for the three investigated peptides, which prompted an analysis of their compactness based on their gyration radius. The results are presented in **Figure 8**, which demonstrates that, despite their inherent flexibility, R5MAP4 and R8MAP8 exhibit sharply defined Gaussian distributions, centered at 13.6 Å and

21.7 Å, respectively. In contrast, the gyration radius distribution for R20 differs from a Gaussian shape, and is more diffuse, indicating a less globular and more fluctuating conformation. Thus, the present molecular dynamics study establishes that while R5MAP4 and R8MAP8 exhibit globular shapes with distinct radii, R20 has a comparatively less globular structure.

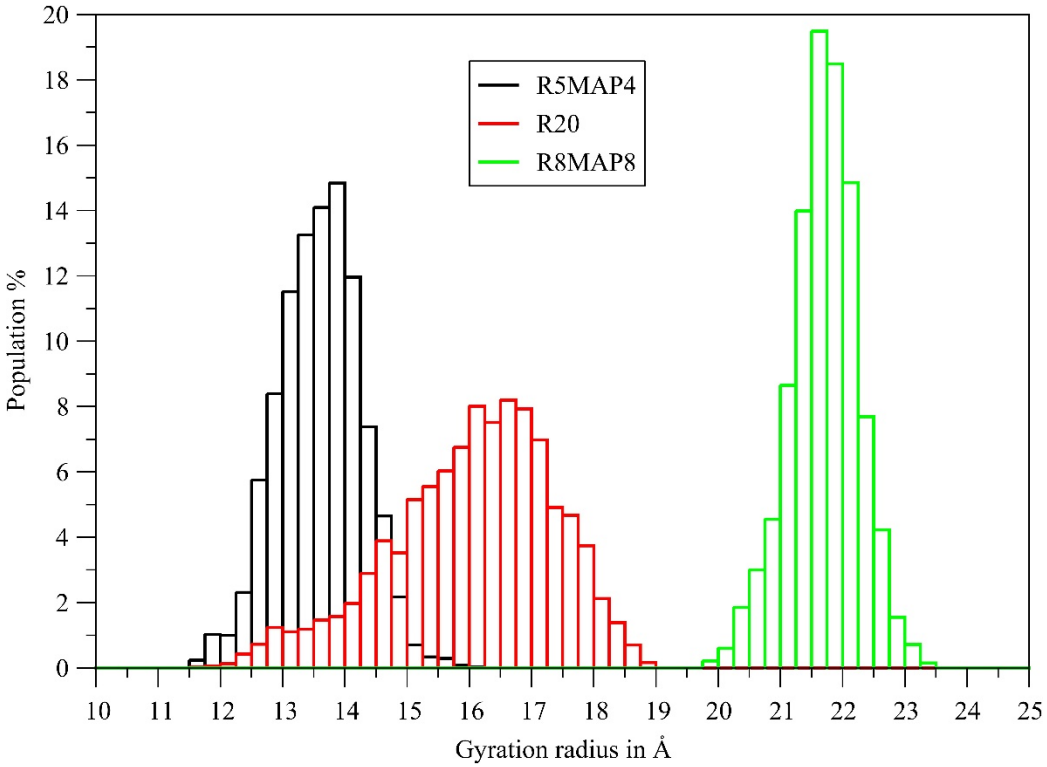

Figure 8. Distribution of gyration radius for R5MAP4, R20 and R8MAP8 determined from MD in water boxes.

2.c.2. Peptides in interaction with bacterial membranes

While the peptides exhibited distinct behavior in terms of their radius of gyration, this alone is not sufficient to explain their differences in antibacterial activity. Therefore, an investigation of the adsorption of R20, R5MAP4 and R8MAP8 peptides was conducted through MD with the membranes of two bacterial strains, *Pseudomonas aeruginosa* (PA, a Gram positive pathogen) and *Staphylococcus aureus* (SA, a Gram negative pathogen), to decipher the mechanism of their

antibacterial activities. It must be emphasized that, with these simulations, it could not be expected to observe membrane permeabilization, pore formation or destruction as this is likely to occur over longer timescales and with the combined action of multiple peptides. Therefore, the focus was only on the initial stage of adsorption, hypothesizing that the more a peptide perturbs the membrane on its own, the stronger is its antibacterial activity. Each membrane system was subjected to a MD simulation time of 1.2 μs in its aqueous and ionic environment and ensuring that each membrane was equilibrated, as confirmed by the convergence of the area per lipid (APL) versus time (**Figure S5**). Interestingly, the convergence was reached before 200 ns for the SA membrane but was only attained after around 350 ns for the PA membrane which can be explained by the fact that SA contains only oleic lipid tails whereas PA contains palmitic and oleic which thus require more simulation times to obtain the equilibrated state.

Subsequently, the peptides R20, R5MAP4, and R8MAP8 were placed above the surfaces of the membranes, and an additional 1.2 μs of MD simulations were conducted. Notably, all peptides were observed to adsorb onto the membranes during the first 200 ns of simulation. This was evidenced for all the four replicas indicating the reproducibility of this phenomenon. To elucidate and quantify the impact of peptide adsorption, we examined classical metrics of membrane perturbation, namely APL and deuterium order parameter (SCD) which were computed after 1 μs to ensure the equilibration of the systems.

When peptides adsorb onto a membrane surface, the APL value is changed and it is considered that the more it moves away from the reference value, the more the impact of the peptide on the integrity of the membrane is consequent [43]. **Table 1** lists the average values of APL along with their standard deviations for PA and SA membranes alone and with R20, R5MAP4, and R8MAP8 peptides.

Table 1. Area per lipid average values, in Å², and standard deviations compiled for membrane alone and complexed with peptides. Computations are made for the equilibrated part of the systems, i.e. the last 200 ns. Values are for P. aeruginosa (PA) and S. aureus (SA) bacteria.

	PA [Å²]	SA [Å²]
Membrane alone	8.72 ± 0.06	11.52 ± 0.12
R20	8.92 ± 0.07	11.55 ± 0.11
R5MAP4	9.26 ± 0.07	12.25 ± 0.11
R8MAP8	8.88 ± 0.06	11.60 ± 0.13

Based on the values presented in **Table 1**, the following information can be extracted: all peptides appear to have an impact on membrane organization. However, the peptide R5MAP4 significantly disrupts PA and SA membranes to a greater extent. It should be noted that for SA, the impact of R20 and R8MAP8 is more moderate compared to PA, where a significant change in behavior is observed. All these findings suggest that the three peptides have differential effects on the membrane properties, with R5MAP4 having a greater influence on lipid packing compared to R8MAP8 and R20.

The observation of such behavior is interestingly correlated with the analyses of SCD as shown on **Figure 9**. These figures are shown individually as supplementary information in **Figures S6 to S11**. In fact, SCD reflects the orientation and mobility of the lipid acyl chains (**Figure S4**). So that any change characterizes the effects of peptides interactions on membranes [44]. A decrease in this parameter indicates significant disorganization of lipids, and is indicative of the strength of

the effect on the membrane. In this context, with regard to PA and SA, the study finds that R5MAP4 has the strongest impact on lipid organization, which is correlated with its biological activity. In the case of SA, both R8MAP8 and R20 have a moderate, yet observable, effect, with no distinction between them being possible. On the other hand, in the case of PA, there is a more notable effect from R8MAP8 and R20, which is consistent with the measurements of APL. It is noteworthy that the phospholipids, namely DOPE for PA, and DOPG and DOPC for SA, feature an oleoyl-type lipid containing a double bond. This double bond naturally introduces disorder into the membrane, which is manifested by a drastic decrease in the lipid tail order parameter (SCD) specifically at carbons 10 and 11.

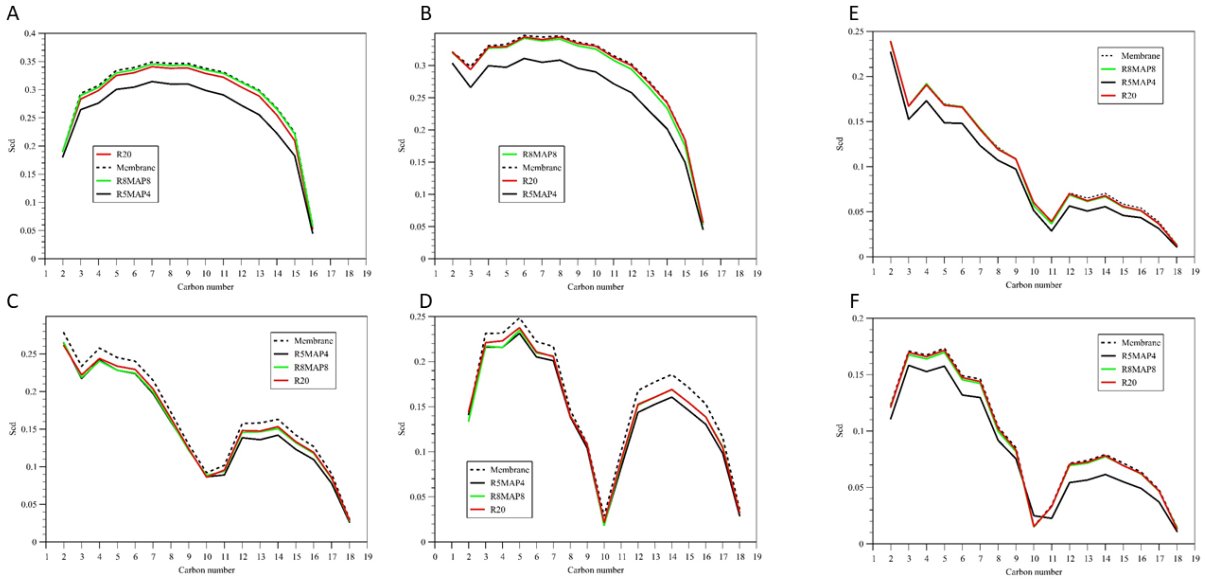

Figure 9. Order parameter (SCD) of lipid bilayers without (dash line) or in the presence of R5MAP4 (black), R8MAP8 (green) and R20 (red) peptides. For *P. aeruginosa*, A and B represent the SN-1 and SN-2 of palmitic lipids, respectively, whereas C and D represent the SN-1 and SN-2 of oleic lipid, respectively. For *S. aureus*, where only the oleic lipid tail exists, E and F refer to the SN-1 and SN-2 of this lipid.

The structural analyses of the R20, R5MAP4 and R8MAP8 interaction with PA and SA membranes are illustrated on **Figure 10**. It is noteworthy that all peptides lie completely on the surface of membranes except for R8MAP8 on the SA membrane. On the latter, R8MAP8 presents two of its chains composed of 8 arginine residues that do not interact with the membrane and remain exposed to the solvent. This observation is not random as it occurs for all 4 replicas of this simulation and it is important to note that the R8MAP8 peptide has sufficient space to lie completely on the SA membrane. We note that for the bacterium PA, R8MAP8 manages to lie completely on its membrane. This phenomenon can be explained by the fact that the SA membrane is distinct from that of PA by their polar heads. Specifically, PA contains the polar heads 3-phosphoethanolamine (PE) and 3-phosphoglycerol (PGR) while SA contains the polar heads 3-phosphocholine (PC) and PGR. Since PC is neutral while PE is negative, this induces a stronger electrostatic field for PA than for SA, resulting in a stronger electrostatic attraction and complete adsorption of R8MAP8 to PA.

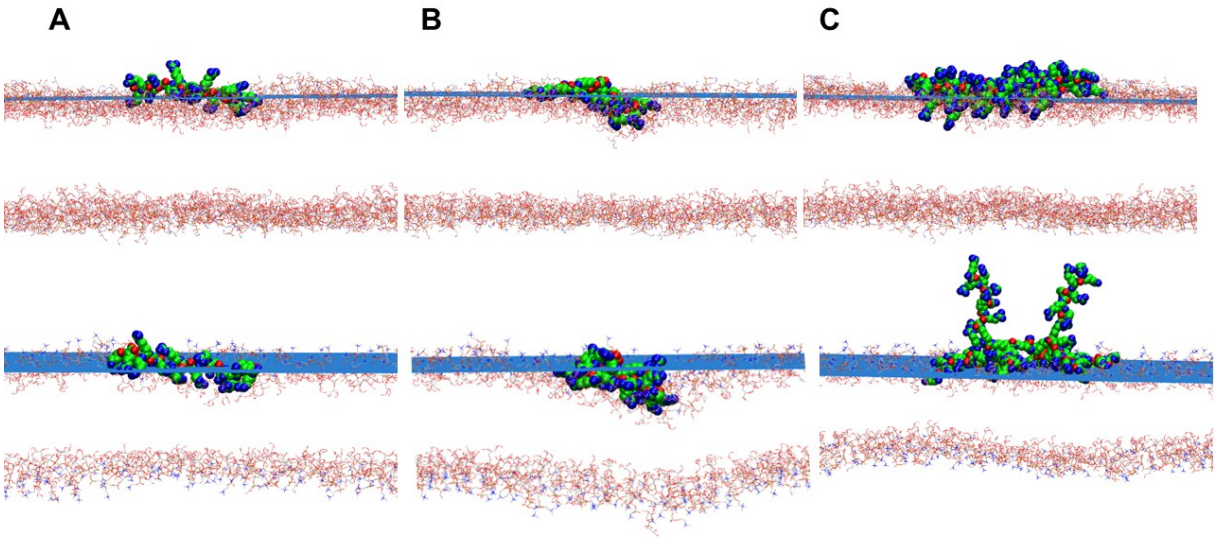

Figure 10. Structural interactions of R20 (A), R5MAP4 (B) and R8MAP8 (C) with the PA (top) and SA (bottom) membranes. For the sake of clarity, water, ions, lipid tails and hydrogens are not

displayed. Peptides are presented with VDW spheres whereas the head of phospholipids moieties are with lines. To localize easily the average position of the upper membrane leaf a plane is displayed in blue.

For our peptides, the antimicrobial activity should result from the disruption of the bacterial membrane. To easily visualize this phenomenon, the average position of the upper membrane leafs are displayed in **Figure 10** to identify the peptide parts which deeply affect the membrane organization. All peptides establish electrostatic interactions with their positively charged arginine residues and the polar heads of phospholipids. However, depending on their topology and structural organization, different behaviors are observed. The R8MAP8 and R20 peptides do not penetrate deeply into the membrane and remain on a surface, which induces a minor perturbation. In contrast, R5MAP4 shows a more pronounced effect with a strong penetration into the membranes, as easily observed in **Figure 10**. This behavior is notably similar for both studied bacteria. This biological activity echoes the gyration radius measurements, where R5MAP4 presents a spherical organization, like R8MAP8, unlike R20 with a smaller radius than R8MAP8. Our results demonstrate that biological activity is not directly correlated with the number of positive charges, i.e., the number of arginine residues, but with a distinct structural organization on the membrane. Thus, R5MAP4, with its spherical aspect and charge density, exerts a stronger constraint on bacterial membranes, inducing better antimicrobial activity.

3. Conclusion and perspectives

Previously we showed that the size of linear poly (L-arginine) has strong effect on the MIC and antibacterial properties of the peptide. With this current work, we presented that the shape and

configuration of the polypeptide has also an impact on the antibacterial properties of the molecule. Some MAP peptides show higher antibacterial properties than a linear peptide for the same number of arginine residues. Moreover, the molecular simulation demonstrated that this antibacterial activity was due to the adsorption/interaction of the peptide to the bacterial membrane and that the mechanical deformation of the bacterial membrane was much higher with a MAP peptide than a linear one. Besides, bigger molecules with longer arms do not present better antibacterial properties even though the number of positive charges is higher. The molecular simulation shows indeed that the spherical structure of bigger molecules is more compact and due to steric hindrance, the peptide cannot lay down to the bacteria surface. Thus, the molecular dynamic simulation helped us to understand the difference in the mechanism of a linear and a MAP peptide.

Now that we proved that there is difference in the antibacterial activities between linear and MAP peptides, the further step is to add MAP peptides in biomaterials, such as multilayer coatings or hydrogels to see the effect on antibacterial properties and to see if these properties can be improved by the addition of these small peptides.

Acknowledgment

This work is funded by the European Union under grant agreement number 101058554 (EIC Accelerator-SPARTHACUS), by BPI (French Public Bank of Investment) ADD (Aide Deep Tech program No 3981662) and from the Région Grand Est through the ERMES project.

References[1] CDC, HAI and Antibiotic Use Prevalence Survey. <https://www.cdc.gov/hai/eip/antibiotic-use.html>, 2022 June 2022).
[2] CDC, Data Portal: From the HAI Hospital Prevalence Survey. <https://www.cdc.gov/hai/data/portal/index.html>, 2015 (accessed June 2022.2022).
[3] W.H. Organization, Antimicrobial resistance. <https://www.who.int/news-room/fact-sheets/detail/antimicrobial-resistance>, 2021 January 2023).
[4] M. Frieri, K. Kumar, A. Boutin, Antibiotic resistance, J. Infect. Public. Health. 10(4) (2017) 369-378. https://doi.org/10.1016/j.jiph.2016.08.007
[5] B. Mehrjou, Y. Wu, P. Liu, G. Wang, P.K. Chu, Design and Properties of Antimicrobial Biomaterials Surfaces, Adv. Healthc. Mater. (2022) 2202073. https://doi.org/10.1002/adhm.202202073
[6] M. Pasupuleti, A. Schmidtchen, M. Malmsten, Antimicrobial peptides: key components of the innate immune system, Crit. Rev. Biotechnol. 32(2) (2012) 143-71. https://doi.org/10.3109/07388551.2011.594423
[7] J.Y. Niu, I.X. Yin, W.K.K. Wu, Q.L. Li, M.L. Mei, C.H. Chu, Antimicrobial peptides for the prevention and treatment of dental caries: A concise review, Arch. Oral Biol. 122 (2021) 105022. https://doi.org/10.1016/j.archoralbio.2020.105022.
[8] G.M. Bohpale, Antimicrobial Peptides: A Promising Avenue for Human Healthcare, Curr. Pharma. Biotech. 21 (2020) 90-96. https://doi.org/10.2174/1389201020666191011121722
[9] J. Shen, G.C. Gurtner, L. Cegelski, Y.P. Yang, Mechanisms of Action and Chemical Origins of Biologically Active Antimicrobial Polymers, 2020. https://doi.org/10.1007/978-3-030-34475-7_13
[10] S. Li, L. Wang, J. Zhang, Z. Zhao, W. Yu, Z. Tan, P. Gao, X. Chen, Combination of natural polyanions and polycations based on interfacial complexation for multi-functionalization of wound dressings, Front. Bioeng. Biotechnol. 10 (2022) 1006584.https://doi.org/10.3389/fbioe.2022.1006584
[11] A. Chen, H. Peng, I. Blakey, A.K. Whittaker, Biocidal Polymers: A Mechanistic Overview, Polym. Rev. 57(2) (2016) 276-310. https://doi.org/10.1080/15583724.2016.1223131

[12] A.S. Abd-El-Aziz, C. Agatemor, N. Etkin, D.P. Overy, M. Lanteigne, K. McQuillan, R.G. Kerr, Antimicrobial Organometallic Dendrimers with Tunable Activity against Multidrug-Resistant Bacteria, Biomacromolecules 16(11) (2015) 3694-703.https://doi.org/ 10.1021/acs.biomac.5b01207
[13] M. Stach, T.N. Siriwardena, T. Kohler, C. van Delden, T. Darbre, J.L. Reymond, Combining topology and sequence design for the discovery of potent antimicrobial peptide dendrimers against multidrug-resistant Pseudomonas aeruginosa, Angew. Chem., Int. Ed. Engl. 53(47) (2014) 12827-31. https://doi.org/10.1002/anie.201409270
[14] T.N. Siriwardena, M. Stach, R. He, B.H. Gan, S. Javor, M. Heitz, L. Ma, X. Cai, P. Chen, D. Wei, H. Li, J. Ma, T. Kohler, C. van Delden, T. Darbre, J.L. Reymond, Lipidated Peptide Dendrimers Killing Multidrug-Resistant Bacteria, J. Am. Chem. Soc. 140(1) (2018) 423-432. https://doi.org/10.1021/acscentsci.0c01135
[15] A.I. Khan, S. Nazir, A. Ullah, M.N.U. Haque, R. Maharjan, S.U. Simjee, H. Olleik, E. Courvoisier-Dezord, M. Maresca, F. Shaheen, Design, Synthesis and Characterization of [G10a]-Temporin SHa Dendrimers as Dual Inhibitors of Cancer and Pathogenic Microbes, Biomolecules 12(6) (2022).https://doi.org/10.3390/biom12060770
[16] J.L. Reymond, Peptide Dendrimers: From Enzyme Models to Antimicrobials and Transfection Reagents, Chimia 75(6) (2021) 535-538. https://doi.org/10.2533/chimia.2021.535
[17] S. Alfei, D. Caviglia, Prevention and Eradication of Biofilm by Dendrimers: A Possibility Still Little Explored, Pharmaceutics 14 (2022) 2016.https://doi.org/10.3390/pharmaceutics14102016
[18] L. Bracci, C. Falciani, B. Lelli, L. Lozzi, Y. Runci, A. Pini, M.G. De Montis, A. Tagliamonte, P. Neri, Synthetic peptides in the form of dendrimers become resistant to protease activity, J. Biol. Chem. 278(47) (2003) 46590-5. https://doi.org/ 10.1074/jbc.M308615200
[19] L. Seon, P. Lavalle, P. Schaaf, F. Boulmedais, Polyelectrolyte Multilayers: A Versatile Tool for Preparing Antimicrobial Coatings, Langmuir 31(47) (2015) 12856-72. https://doi.org/10.1021/acs.langmuir.5b02768
[20] A. Mutschler, L. Tallet, M. Rabineau, C. Dollinger, M.-H. Metz-Boutigue, F. Schneider, B. Senger, N.E. Vrana, P. Schaaf, P. Lavalle, Unexpected Bactericidal Activity of Poly(arginine)/Hyaluronan Nanolayered Coatings, Chem. Mater. 28(23) (2016) 8700-8709. https://doi.org/10.1021/acs.chemmater.6b03872
[21] A. Mutschler, C. Betscha, V. Ball, B. Senger, N.E. Vrana, F. Boulmedais, A. Schroder, P. Schaaf, P. Lavalle, Nature of the Polyanion Governs the Antimicrobial Properties of Poly(arginine)/Polyanion Multilayer Films, Chem. Mater. 29(7) (2017) 3195-3201. https://doi.org/ 10.1021/acs.chemmater.7b00334
[22] J.T. Mika, G. Moiset, A.D. Cirac, L. Feliu, E. Bardaji, M. Planas, D. Sengupta, S.J. Marrink, B. Poolman, Structural basis for the enhanced activity of cyclic antimicrobial peptides: the case of BPC194, Biochim. Biophys. Acta 1808(9) (2011) 2197-205. https://doi.org/10.1016/j.bbamem.2011.05.001
[23] D.W. Lee, B.S. Kim, Antimicrobial cyclic peptides for plant disease control, Plant Pathol. J. 31(1) (2015) 1-11. https://doi.org/ 10.5423/PPJ.RW.08.2014.0074
[24] V.G. Joshi, V.D. Dighe, D. Thakuria, Y.S. Malik, S. Kumar, Multiple antigenic peptide (MAP): a synthetic peptide dendrimer for diagnostic, antiviral and vaccine strategies for emerging and re-emerging viral diseases, Indian. J. Virol. 24(3) (2013) 312-20. https://doi.org/ 10.1007/s13337-013-0162-z

[25] C. Almazan, L. Simo, L. Fourniol, S. Rakotobe, J. Borneres, M. Cote, S. Peltier, J. Maye, N. Versille, J. Richardson, S.I. Bonnet, Multiple Antigenic Peptide-Based Vaccines Targeting Ixodes ricinus Neuropeptides Induce a Specific Antibody Response but Do Not Impact Tick Infestation, Pathogens 9(11) (2020) 900. https://doi.org/ 10.3390/pathogens9110900
[26] T. Verma, A. Aggarwal, S. Singh, S. Sharma, S.J. Sarma, Current challenges and advancements towards discovery and resistance of antibiotics, J. Mol. Struct. 1248 (2022) 131380. https://doi.org/10.1016/j.molstruc.2021.131380
[27] R. Rai, S. Dubey, K.V. Santosh, A. Biswas, V. Mehrotra, D.N. Rao, Design and synthesis of multiple antigenic peptides and their application for dengue diagnosis, Biologicals 49 (2017) 81-85. https://doi.org/10.1016/j.biologicals.2017.08.005
[28] S. Harm, K. Lohner, U. Fichtinger, C. Schildbock, J. Zottl, J. Hartmann, Blood Compatibility-An Important but Often Forgotten Aspect of the Characterization of Antimicrobial Peptides for Clinical Application, Int. J. Mol. Sci. 20(21) (2019) 5426. https://doi.org/10.3390/ijms20215426
[29] R. Salomon-Ferrer, A.W. Gotz, D. Poole, S. Le Grand, R.C. Walker, Routine Microsecond Molecular Dynamics Simulations with AMBER on GPUs. 2. Explicit Solvent Particle Mesh Ewald, J. Chem. Theory Comput. 9(9) (2013) 3878-88. https://doi.org/10.1021/ct400314y
[30] A. Jakalian, D.B. Jack, C.I. Bayly, Fast, efficient generation of high-quality atomic charges. AM1-BCC model: II. Parameterization and validation, J. Comput. Chem. 23(16) (2002) 1623-41. https://doi.org/10.1002/jcc.10128
[31] W.L. Jorgensen, J. Chandrasekhar, J.D. Madura, R.W. Impey, M.L. Klein, Comparison of simple potential functions for simulating liquid water, J. Chem. Phys. 79(2) (1983) 926-935. https://doi.org/10.1063/1.445869
[32] J.A. Maier, C. Martinez, K. Kasavajhala, L. Wickstrom, K. Hauser, C. Simmerling, ff14SB: Improving the accuracy of protein side chain and backbone parameters from ff99SB, J. Chem. Theory Comput. 11(8) (2015) 3696-3713. https://doi.org/10.1021/acs.jctc.5b00255
[33] D. Vassetti, M. Pagliai, P. Procacci, Assessment of GAFF2 and OPLS-AA General Force Fields in Combination with the Water Models TIP3P, SPCE, and OPC3 for the Solvation Free Energy of Druglike Organic Molecules, J. Chem. Theory Comput. 15(3) (2019) 1983-1995. https://doi.org/10.1021/acs.jctc.8b01039
[34] C.J. Dickson, R.C. Walker, I.R. Gould, Lipid21: Complex Lipid Membrane Simulations with AMBER, J Chem Theory Comput 18(3) (2022) 1726-1736. https://doi.org/10.1021/acs.jctc.1c01217
[35] S. Jo, T. Kim, V.G. Iyer, W. Im, CHARMM-GUI: a web-based graphical user interface for CHARMM, J. Comput. Chem. 29(11) (2008) 1859-65. https://doi.org/10.1002/jcc.20945
[36] A. Li, J.W. Schertzer, X. Yong, Molecular dynamics modeling of Pseudomonas aeruginosa outer membranes, Phys. Chem. Chem. Phys. 20(36) (2018) 23635-23648. https://doi.org/10.1039/C8CP04278K
[37] T. Zhang, Y. Qiu, Q. Luo, L. Zhao, X. Yan, Q. Ding, H. Jiang, H. Yang, The Mechanism by Which Luteolin Disrupts the Cytoplasmic Membrane of Methicillin-Resistant Staphylococcus aureus, J. Phys. Chem. B. 122(4) (2018) 1427-1438. https://doi.org/10.1021/acs.jpcb.7b05766
[38] D.R. Roe, T.E. Cheatham, 3rd, PTRAJ and CPPTRAJ: Software for Processing and Analysis of Molecular Dynamics Trajectory Data, J. Chem. Theory. Comput. 9(7) (2013) 3084-95. https://doi.org/10.1021/ct400341p
[39] W. Humphrey, A. Dalke, K. Schulten, VMD: Visual Molecular Dynamics, J. Mol. Graph. 14(1) (1996) 33-38. https://doi.org/10.1016/0263-7855(96)00018-5

[40] M. Hyldgaard, T. Mygind, B.S. Vad, M. Stenvang, D.E. Otzen, R.L. Meyer, The Antimicrobial Mechanism of Action of Epsilon-Poly-L-Lysine, Appl. Environ. Microbiol. 80(16) (2014) 7758-7770. https://doi.org/ 10.1128/AEM.02204-14
[41] V. Gribova, L. Petit, L. Kocgozlu, C. Seguin, S. Fournel, A. Kichler, N.E. Vrana, P. Lavalle, Polyarginine as a Simultaneous Antimicrobial, Immunomodulatory, and miRNA Delivery Agent within Polyanionic Hydrogel, Macromol. Biosci. 22(6) (2022) 2200043. https://doi.org/ 10.1002/mabi.202200043
[42] H. Ozcelik, N.E. Vrana, A. Gudima, V. Riabov, A. Gratchev, Y. Haikel, M.H. Metz-Boutigue, A. Carrado, J. Faerber, T. Roland, H. Kluter, J. Kzhyshkowska, P. Schaaf, P. Lavalle, Harnessing the multifunctionality in nature: a bioactive agent release system with self-antimicrobial and immunomodulatory properties, Adv. Healthc. Mater. 4(13) (2015) 2026-36. https://doi.org/10.1002/adhm.201500546
[43] G. Shahane, W. Ding, M. Palaiokostas, M. Orsi, Physical properties of model biological lipid bilayers: insights from all-atom molecular dynamics simulations, J. Mol. Model. 25(3) (2019) 76. https://doi.org/ 10.1007/s00894-019-3964-0[44] S. Moradi, A. Nowroozi, M. Shahlaei, Shedding light on the structural properties of lipid bilayers using molecular dynamics simulation: a review study, RSC Adv. 9(8) (2019) 4644-4658. https://doi.org/10.1039/c8ra08441f